Article:
Dong, A, Sun, Z, Kendall, B et al. (9 more authors) (2022) Insights from modern diffuse-flow hydrothermal systems into the origin of post-GOE deep-water Fe-Si precipitates. Geochimica et Cosmochimica Acta, 317. pp. 1-17. ISSN 0016-7037

https://doi.org/10.1016/j.gca.2021.10.001

Supplementary Material:

Insights from Modern Diffuse Flow Hydrothermal Systems into the origin of post-GOE Deep-water Fe-Si Precipitates

Aiguo Dong, Zhilei Sun*, Brian Kendall, Gareth Izon, Hong Cao, Zhihong Li, Xiaoming Ma, Xijie Yin, Zhen Qiu, Xiang-kun Zhu, Andrey Bekker, Simon W. Poulton

* Corresponding author.

E-mail: zhileisun@yeah.net

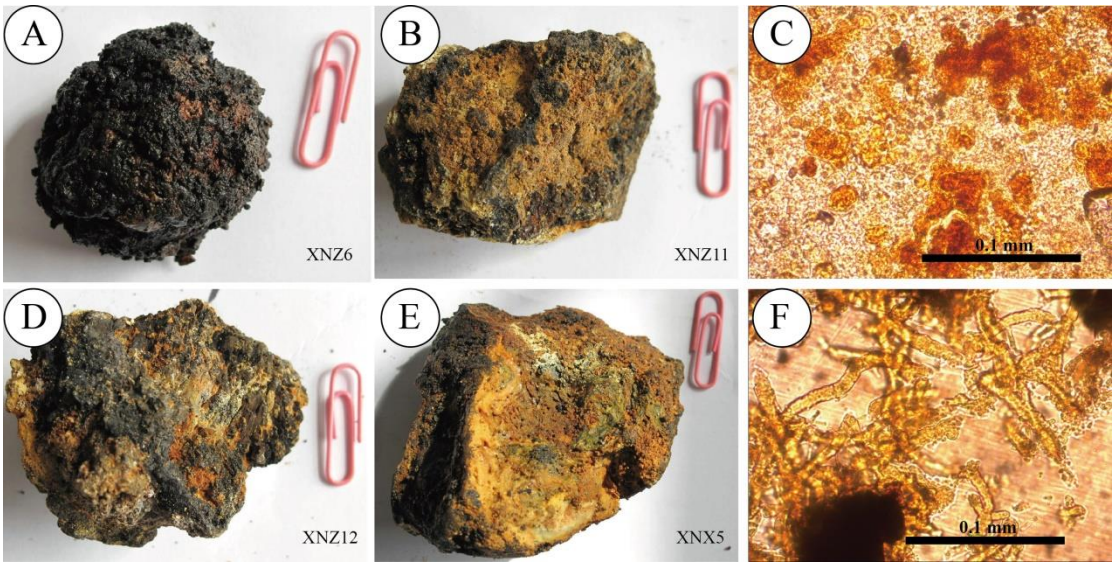

Fig. S1. Hand-specimen photographs (A–B, D–E) and photomicrographs (C, F) of typical Fe-Si precipitates from the SWIR. Sample identifiers are in the bottom-right corner of the photographs and the paperclip (15 mm long) provides scale. Photomicrographs C and F correspond to samples XNZ11 and XNZ7, respectively.

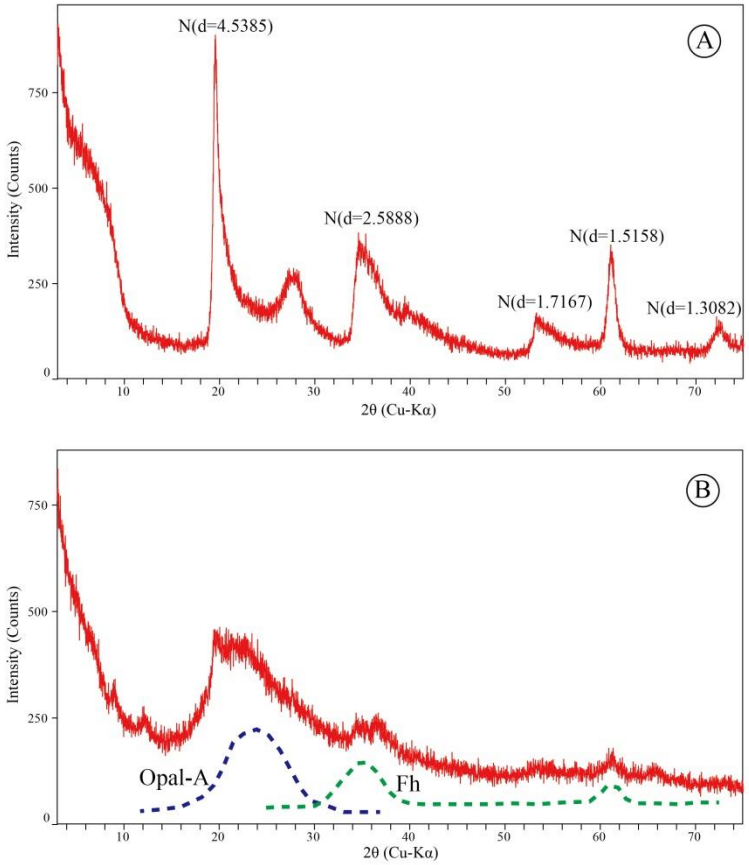

Fig. S2. X-ray diffraction patterns of hydrothermal Fe-Si precipitates from the SWIR. Panels **A** and **B** display respective spectra from F-N- (XNZ10) and F-O-type (XNZ1) samples. Peaks labelled *N* in panel **A** are typical for the mineral nontronite. The green and blue dashed lines in panel **B** represent idealised spectra of 2-line-ferrihydrite (Fh) and opal-A, respectively.

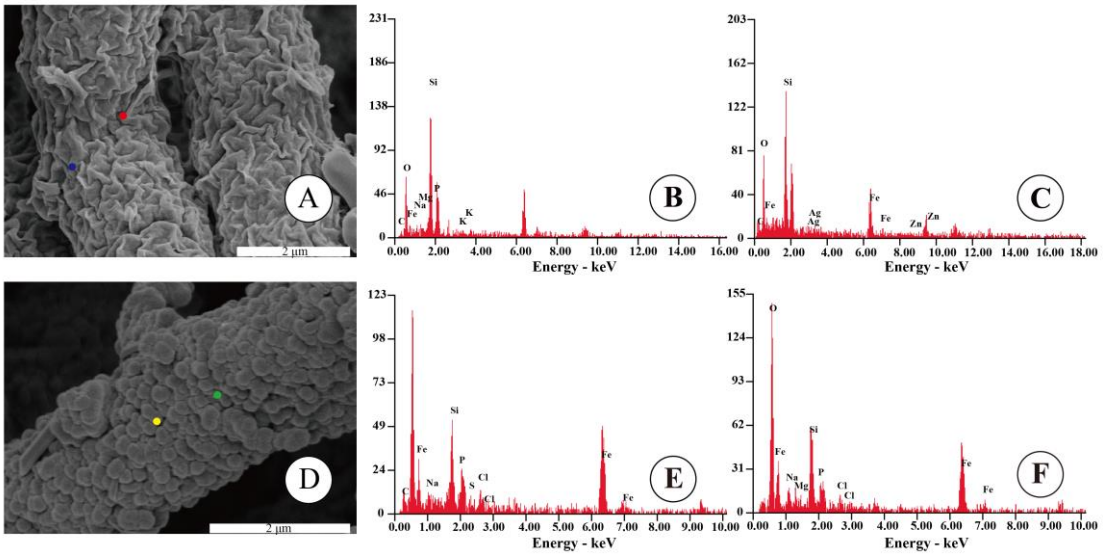

Fig. S3. Scanning electron photomicrographs (A, D) and EDS-derived elemental abundance data (B–C, E–F) obtained from selected SWIR Fe-Si precipitates. Representative F-N- (XNZ10) and F-O-type (XNZ1) samples are pictured in panels **A** and **D**, respectively. The EDS data in panels **B, C**, **E** and **F** correspond to spot analyses located in panels **A** and by the retrospective red, blue, green and yellow circles.

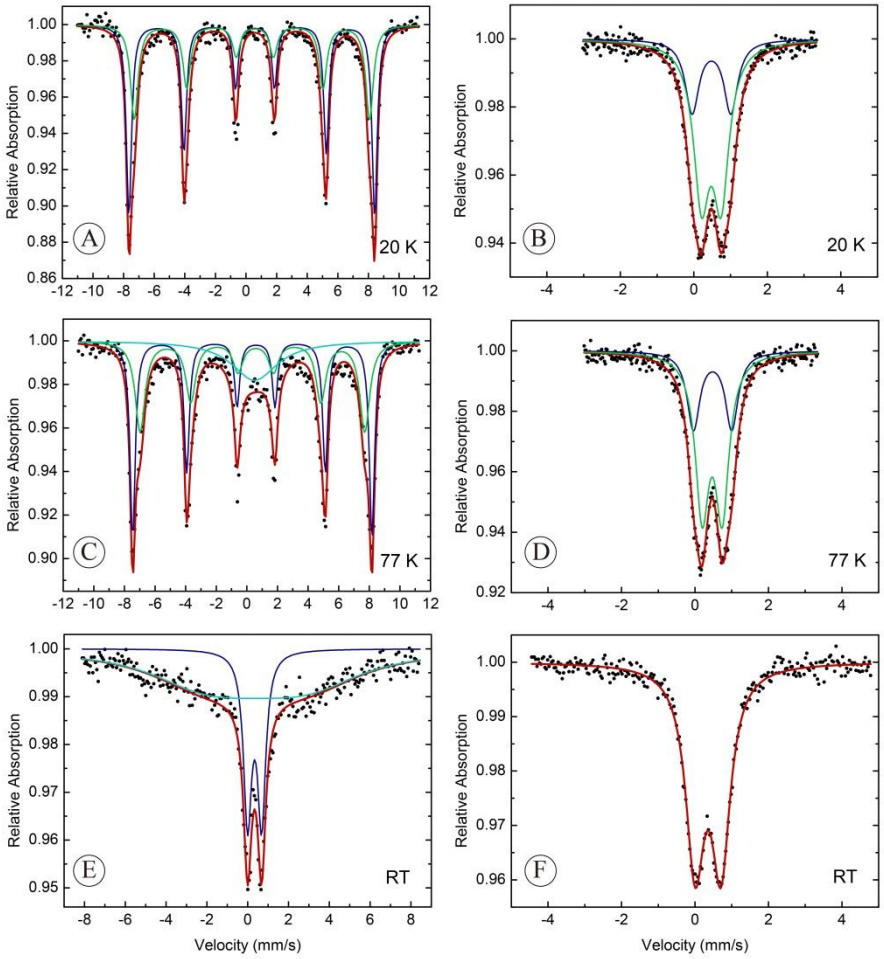

Fig. S4. Mössbauer spectra of Fe-Si precipitates from the SWIR. The left bank of panels (**A, C, E**) illustrate spectra from an F-O-type sample (XNZ1) from the Longqi Hydrothermal Field, while the right bank of panels (**B, D, F**) are sourced from a F-N-type sample (XNX1) from the Duanqiao Hydrothermal Field. Analysis temperatures are given in Kelvin (K) in the bottom-right of each panel. RT abbreviates room temperature. The black points are analytical data. The green and blue lines represent different sub-spectra, while the red line represents the total fit derived from MossWinn.

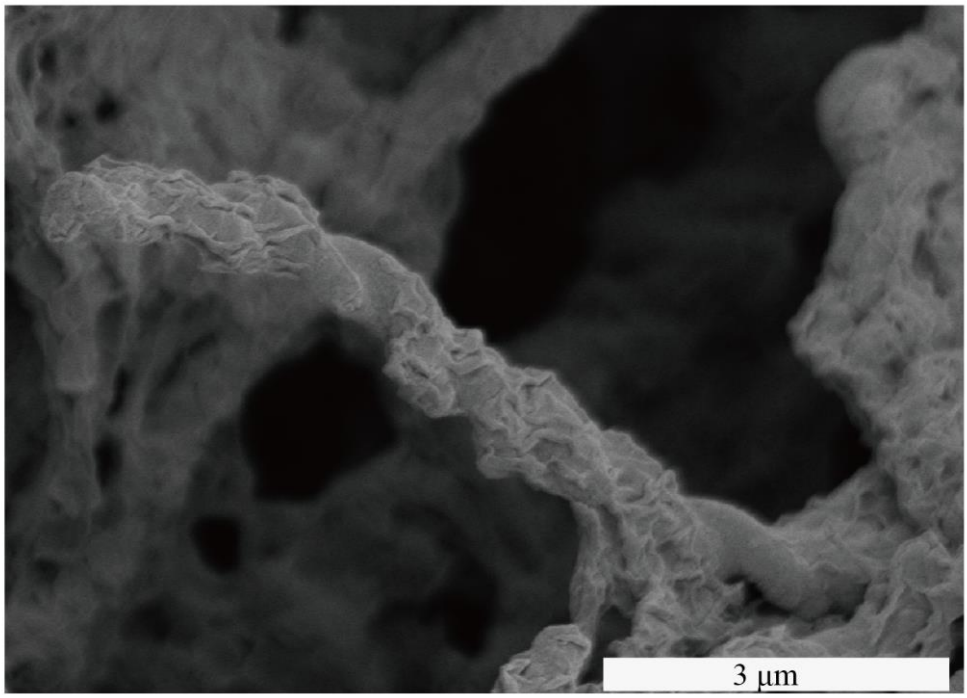

Fig. S5. A scanning electron photomicrograph showing a slightly altered twisted filament observed within a F-O-type (XNZ1) sample from the SWIR.

Table S1: Sample locations and related information.

Sample I.D	Type	Dominant Mineral	Hydrothermal Field	Station	Date	Longitude	Latitude	Depth	Distance*
						(ºS)	(ºE)	(m)	(m)
XNS1	F-N type Fe-Si precipitate	nontronite, ferrihydrite	Tiancheng	20VII-S25-TVG21	2009-02-22	63.5414	27.9506	3668	11.91
XNS2	F-N type Fe-Si precipitate	nontronite, ferrihydrite	Tiancheng	20V-S31-TVG13	2009-02-22	63.5560	27.9558	3851	1540
XNZ3	F-N type Fe-Si precipitate	nontronite, ferrihydrite	Duanqiao	20V-S17-TVG7	2008-12-04	50.4672	37.6586	1740	128.6
XNZ6	F-N type Fe-Si precipitate	nontronite, ferrihydrite	Duanqiao	20V-S18-TVG8	2008-12-04	50.4678	37.6587	1745	155.7
XNZ10	F-N type Fe-Si precipitate	nontronite, ferrihydrite	Duanqiao	20V-S20-TVG10	2008-12-04	50.4682	37.6589	1759	192.7
XNZ11	F-N type Fe-Si precipitate	nontronite, ferrihydrite	Duanqiao	20V-S32-TVG8	2008-12-13	50.4671	37.6579	1739	50.4
XNX1	F-N type Fe-Si precipitate	nontronite, ferrihydrite	Longqi	20V-S7-TVG2	2008-11-24	49.6494	49.6494	2795	N.D.
XNX3	F-N type Fe-Si precipitate	nontronite, ferrihydrite	Longqi	20V-S31-TVG13	2008-11-24	49.6669	37.7787	2930	1560
XNX4	F-N type Fe-Si precipitate	nontronite, ferrihydrite	Longqi	20V-S31-TVG13	2008-11-24	49.6669	37.7787	2930	1560
XNX6	F-N type Fe-Si precipitate	nontronite, ferrihydrite	Longqi	20VI-S16-TVG13	2009-01-16	49.6474	37.7805	2786	359.8
XNZ1	F-O type Fe-Si precipitate	opal-A, ferrihydrite	Duanqiao	20V-S17-TVG7	2008-12-04	50.4672	37.6586	1740	128.6
XNZ2	F-O type Fe-Si precipitate	opal-A, ferrihydrite	Duanqiao	20V-S17-TVG7	2008-12-04	50.4672	37.6586	1740	128.6
XNZ4	F-O type Fe-Si precipitate	opal-A, ferrihydrite	Duanqiao	20V-S17-TVG7	2008-12-04	50.4672	37.6586	1740	128.6
XNZ5	F-O type Fe-Si precipitate	opal-A, ferrihydrite	Duanqiao	20V-S17-TVG7	2008-12-04	50.4672	37.6586	1740	128.6
XNZ7	F-O type Fe-Si precipitate	opal-A, ferrihydrite	Duanqiao	20V-S19-TVG8	2008-12-04	50.4627	37.6468	1760	1244
XNZ8	F-O type Fe-Si precipitate	opal-A, ferrihydrite	Duanqiao	20V-S19-TVG8	2008-12-04	50.4627	37.6468	1760	1244
XNZ9	F-O type Fe-Si precipitate	opal-A, ferrihydrite	Duanqiao	20V-S20-TVG10	2008-12-04	50.4682	37.6589	1759	192.7
XNZ12	F-O type Fe-Si precipitate	opal-A, ferrihydrite	Duanqiao	20V-S32-TVG8	2008-12-13	50.4671	37.6579	1739	50.4
XNZ13	F-O type Fe-Si precipitate	opal-A, ferrihydrite	Duanqiao	20V-S32-TVG8	2008-12-13	50.4671	37.6579	1739	50.4
XNX2	F-O type Fe-Si precipitate	opal-A, ferrihydrite	Longqi	20V-S7-TVG2	2008-11-24	49.6494	49.6494	2795	N.D.

XNX5	F-O type Fe-Si precipitate	opal-A, ferrihydrite	Longqi	20VI-S16-TVG13	2009-01-16	49.6474	37.7805	2786	359.8
XNZ14	Sediments		Duanqiao	20V-S32-TVG14	2008-12-13	50.4671	37.6579	1739	50.4
XNZ15	Sulfide		Duanqiao	20VII-S10-TVG8	2009-02-09	50.4669	37.6575	1719	9.445

*Distance to the nearest vent; N.D. = No Data

Table S2: Temperature dependant Mössbauer parameters of SWIR Fe-Si precipitates.

Sample ID	Temperature (K)	Isomer Shift (mm s^{-1})	*QS (mm s^{-1})	Hyperfine Field T	Line Width (mm s^{-1})	Relative area (%)
XNZ1	RT	0.430(9)	--	19 (1)	6(1)	73.6
		0.338(9)	0.690(9)	--	0.48(2)	24.6
	77	0.478(2)	-0.242(5)	48.61(4)	0.41(1)	43.4
		0.476(7)	-0.22(1)	45.60(1)	0.78(3)	37.7
		0.50(6)	--	--	3.6(3)	19
	20	0.490(2)	-0.216(5)	49.91(4)	0.40(1)	57.9
		0.486(5)	-0.19(1)	47.80(1)	0.60(2)	42.1
XNX1	RT	0.355(3)	0.706(5)	--	0.617(8)	100
	77	0.479(5)	1.04(4)	--	0.42(4)	31.4
		0.467(3)	0.55(3)	--	0.45(2)	68.6
	20	0.481(5)	1.05(4)	--	0.45(4)	29.2
		0.475(3)	0.53(3)	--	0.53(2)	70.8

*QS-quadrupole splitting;

Table S3: Major element, loss-on-ignition, and organic carbon abundances.

Sample	Hydrothermal field	Dominant mineral phase	SiO_2	Al_2O_3	CaO	Fe_2O_3	K_2O	MgO	MnO	Na_2O	P_2O_5	TiO_2	BaO	*LOI	Total	S	C_{org}
			(Wt. %)												(%)	(wt. %)	
XNS1	Tian Zuo	nontronite, ferrihydrite	15.8	0.37	0.96	56.6	0.21	3.89	0.4	0.8	1.26	0.02	0.01	N.D.	N.D.	1.12	0.41
XNS2	Tian Zuo	nontronite, ferrihydrite	13.9	2.49	1.26	44.7	0.15	0.98	0.58	0.45	1.26	0.11	0.07	N.D.	N.D.	7.61	0.42
XNZ3	Duan Qiao	nontronite, ferrihydrite	19.65	0.2	1.04	21	0.68	1.66	25.3	2.39	0.83	0.02	0.06	23.5	96.4	0.1	0.16
XNZ6	Duan Qiao	nontronite, ferrihydrite	13.4	0.34	2.21	29.5	0.74	1.83	23.2	1.46	1.44	0.01	0.36	22.9	97.5	0.03	0.31
XNZ10	Duan Qiao	nontronite, ferrihydrite	48.7	<0.01	0.41	31.1	0.43	2.21	0.35	1.09	0.07	<0.01	0.02	15.5	99.9	<0.01	0.18
XNZ11	Duan Qiao	nontronite, ferrihydrite	8.69	0.06	1.29	11.05	1.01	1.58	46.1	2.02	0.35	0.01	0.19	22.8	95.2	0.46	0.09
XNX1	Long Qi	nontronite, ferrihydrite	17.5	0.14	1.55	28.7	0.73	1.58	20.2	1.39	0.83	0.01	0.85	23	96.6	0.17	0.25
XNX3	Long Qi	nontronite, ferrihydrite	23.4	0.79	1.4	28.3	0.59	1.23	14	1.78	1.16	0.06	0.08	22.47	95.3	0.36	0.32
XNX4	Long Qi	nontronite, ferrihydrite	21.8	1.5	1.62	31.7	0.51	1.36	11.55	1.65	1.38	0.12	0.07	23.06	99.4	0.79	0.63
XNX6	Long Qi	nontronite, ferrihydrite	14.2	0.09	1.73	9.72	1.29	1.81	43.4	1.91	0.16	0.01	0.79	20.1	95.3	0.34	0.09
XNZ1	Duan Qiao	opal-A, ferrihydrite	61.5	0.07	0.28	16.95	0.3	0.72	5.07	0.95	0.44	0.01	0.07	14.25	100.5	0.05	0.14
XNZ2	Duan Qiao	opal-A, ferrihydrite	33.3	0.38	0.8	18.5	0.66	1.22	11.35	6.33	0.62	0.02	0.07	22.18	96.5	0.47	0.17
XNZ4	Duan Qiao	opal-A, ferrihydrite	76.3	0.17	0.34	7.51	0.2	0.24	1.44	2.41	0.29	<0.01	0.02	12.37	101.3	0.09	0.07
XNZ5	Duan Qiao	opal-A, ferrihydrite	81.1	0.03	0.22	6.27	0.13	0.13	0.75	1.22	0.17	<0.01	0.01	10.1	100.1	0.05	0.06
XNZ7	Duan Qiao	opal-A, ferrihydrite	84.6	0.07	0.17	6.43	0.13	0.06	0.21	0.3	0.09	<0.01	0.01	8.73	100.8	0.01	0.07
XNZ8	Duan Qiao	opal-A, ferrihydrite	88.1	0.05	0.12	4.59	0.09	0.05	0.11	0.24	0.07	<0.01	0.01	5.22	98.7	0.01	0.31
XNZ9	Duan Qiao	opal-A, ferrihydrite	37.4	0.19	0.95	25.8	0.47	0.88	12.65	1.48	0.91	0.02	0.05	19.5	100.5	0.08	0.11
XNZ12	Duan Qiao	opal-A, ferrihydrite	79.7	0.09	0.05	10.25	0.19	0.16	0.27	0.17	0.14	<0.01	0.02	9.91	101	0.69	0.15
XNZ13	Duan Qiao	opal-A, ferrihydrite	60.4	0.1	0.26	10.9	0.32	0.43	7.37	1.54	0.17	<0.01	1.7	17.83	101.2	0.47	0.05
XNX2	Long Qi	opal-A, ferrihydrite	61.2	0.03	0.62	17.3	0.15	0.23	4.86	0.78	0.67	<0.01	0.04	14.9	101	0.02	0.24

XNX5	Long Qi	opal-A, ferrihydrite	83.2	0.04	0.26	6.61	0.15	0.27	2.21	0.33	0.1	<0.01	0.05	8.27	101.5	0.14	0.13
XNZ14	Duan Qiao	Sediment	15.85	6.24	2.9	38.8	0.09	2.21	0.1	0.69	0.94	0.2	0.01	N.D.	N.D.	>10.0	N.D.
XNZ15	Duan Qiao	Sulfide	3.29	1.02	0.07	24.9	0.03	0.04	0.06	0.06	0.01	<0.01	0.01	N.D.	N.D.	>10.0	N.D.

* LOI represents loss on ignition

†C_{Org} represents total organic carbon contents.

N.D. = Not Determined

56

57

Table S4: Trace element abundances.

Sample	Li	Be	B	V	Cr	Co	Ni	Ga	Ge	As	Sr	Zr	Ag	Cd	Sb	Cs	Hf	Pb	Th	U
	(mg kg^{-1})																			
XNS1	2.7	0.3	350	422	167	481	91.3	3.7	1.1	144	288	26.1	1.07	0.54	1.79	0.1	0.5	11.5	0.3	10.3
XNS2	1.3	0.1	170	458	56.6	466	16	12.1	3.34	365	138	13.4	8.13	9.8	7.94	0.14	0.4	781	0.3	9.12
XNZ3	139	0.2	130	126	6.19	195	254	7.63	2.44	109	347	3.16	0.24	7.83	4.91	0.05	0.1	10.8	0.1	4.15
XNZ6	104	0.1	200	341	5.65	297	189	7.05	1.84	316	843	6.73	0.07	5.99	6.92	0.21	0.1	128	0.1	4.22
XNZ10	3.5	2.6	30	11	3.3	4.4	3.3	0.22	1.39	9.9	69	2.44	0.13	0.02	0.3	0.13	0.1	2.37	0.7	2.17
XNZ11	353	0.3	60	104	4.67	13	182	19.9	2.35	48	552	2.48	0.04	2.06	6.87	0.08	0	4.92	0.1	4.73
XNX1	162	0.2	200	123	2.71	36	16.7	6.33	1.11	66	1020	1.71	0.07	1.83	5.37	0.1	0	6.47	0	2.21
XNX3	59.7	0.4	160	222	21.5	232	54.2	7.65	2.96	145	394	10.7	0.45	2.67	3.15	0.22	0.3	271	0.2	3.41
XNX4	28.7	0.3	170	289	39.4	414	65.4	8.54	1.9	198	396	14.3	0.92	2.63	3.36	0.3	0.4	379	0.3	4.1
XNX6	91.2	0.2	60	140	3.62	18	332	34.5	5.7	38	896	2.45	0.08	2.09	10.4	0.24	0.1	3.95	0.1	3.01
XNZ1	1.6	0.4	50	45	5.72	27	25	1.96	1.8	62	131	6.66	0.17	0.23	1.11	0.08	0.1	238	0.1	3.15
XNZ2	8.3	0.3	120	114	4.78	77	77.8	3.73	1.25	92	215	5.49	0.34	1.08	3.26	0.08	0.2	213	0.3	3.29
XNZ4	14.1	0.1	40	47	1.57	0.9	5.4	0.94	0.54	37	77.8	1.53	0.02	0.22	1.08	0.08	0.1	4.64	0.2	0.91
XNZ5	9.8	0.1	30	23	1.17	0.6	4	0.21	0.89	20	70.8	0.5	0.02	0.11	0.59	0.08	0	5.76	0.1	0.65
XNZ7	0.9	0.2	20	9	2.03	0.3	1.8	0.31	2.46	7.8	40	0.41	0.02	0.01	0.13	0.31	0	2.55	0.1	0.49
XNZ8	0.6	0.2	10	7	1.61	0.3	1	0.28	1.69	6.4	33.5	0.21	0.02	0.02	0.1	0.19	0	3.39	0	0.64
XNZ9	71.5	0.8	130	176	13.8	19	32.3	4.06	1.61	127	314	1.06	0.15	1.38	3.4	0.09	0	19.2	0	1.44
XNZ12	0.8	0.1	10	44	4.17	1.9	4.5	1.91	4.1	40	23.8	2.47	0.02	0.02	1.78	0.15	0.1	58.2	0.1	6.23
XNZ13	8.5	0.4	40	39	0.64	11	24.1	4.54	4.65	15	738	0.43	0.01	0.09	2.18	0.12	0	2.04	0	3.31
XNX2	26.2	0.1	80	95	4.36	2	11.5	2.19	1.57	83	197	11.8	0.03	0.54	1.94	0.08	0.2	60.3	0.2	2.55
XNX5	5.5	0.3	20	18	3.35	2.8	29.3	1.5	1.3	21	102	2.2	0.06	0.21	1.17	0.06	0.1	4.39	0.1	2.6
XNZ14	1.2	0.2	40	961	139	196	45.7	75.3	21.9	473	49.8	11.4	31.4	16.8	15.9	0.08	0.5	2634	0.2	13.6
XNZ15	0.1	0	<10	11	1.26	0.3	1.9	50.7	8.73	516	3.7	0.47	142	741	45.2	0.07	0	1703	0.1	0.32

Table S5: Rare earth elements abundances.

Sample	La	Ce	Pr	Nd	Sm	Eu	Gd	Tb	Dy	Y	Ho	Er	Tm	Yb	Lu	*TREY	Eu_N/Eu_N^*	Ce_N/Ce_N^*	Pr_N/Pr_N^*	Y/Ho	Sm/Yb
	mg kg^{-1}																				
XNS1	8.92	7.05	1.62	7.17	1.44	0.47	1.89	0.29	1.94	13.23	0.44	1.38	0.19	1.35	0.21	47.59	1.46	0.42	1.22	30.07	1.07
XNS2	4.42	4.78	0.91	4.21	0.96	0.61	1.31	0.22	1.45	9.88	0.34	1.06	0.14	1.02	0.16	31.47	2.69	0.55	1.12	29.06	0.94
XNZ3	N.D.	N.D.	N.D.	N.D.	N.D.	N.D.	N.D.	N.D.	N.D.	N.D.	N.D.	N.D.	N.D.	N.D.	N.D.	N.D.	N.D.	N.D.	N.D.	N.D.	N.D.
XNZ6	3.34	4.87	0.85	4.36	1.10	0.72	1.75	0.27	1.81	11.31	0.39	1.21	0.16	1.04	0.16	33.34	2.69	0.67	1.01	29.00	1.06
XNZ10	0.47	0.71	0.14	0.71	0.19	0.21	0.31	0.05	0.28	2.07	0.06	0.17	0.02	0.14	0.02	5.55	4.39	0.63	1.06	34.50	1.36
XNZ11	0.22	0.34	0.08	0.39	0.08	0.06	0.14	0.02	0.12	0.93	0.03	0.10	0.01	0.09	0.02	2.63	3.06	0.58	1.15	31.00	0.89
XNX1	0.93	0.92	0.20	0.95	0.25	0.18	0.34	0.06	0.46	3.44	0.11	0.36	0.05	0.37	0.06	8.68	2.99	0.49	1.14	31.27	0.68
XNX3	4.95	5.28	0.97	4.43	1.00	0.62	1.37	0.23	1.46	9.22	0.33	1.03	0.14	0.98	0.16	32.17	2.62	0.55	1.12	27.94	1.02
XNX4	5.28	5.60	1.04	4.83	1.15	0.64	1.48	0.26	1.65	10.27	0.38	1.17	0.17	1.09	0.17	35.18	2.37	0.55	1.11	27.03	1.06
XNX6	N.D.	N.D.	N.D.	N.D.	N.D.	N.D.	N.D.	N.D.	N.D.	N.D.	N.D.	N.D.	N.D.	N.D.	N.D.	N.D.	N.D.	N.D.	N.D.	N.D.	N.D.
XNZ1	3.54	4.97	0.77	3.70	0.84	0.54	1.33	0.21	1.40	11.35	0.34	1.07	0.15	0.94	0.16	31.31	2.62	0.69	1.02	33.38	0.89
XNZ2	2.65	4.23	0.67	3.32	0.79	0.62	1.14	0.21	1.34	8.40	0.31	0.94	0.13	0.82	0.14	25.71	3.10	0.73	1.00	27.10	0.96
XNZ4	0.84	1.41	0.19	0.75	0.18	0.10	0.19	0.03	0.21	1.20	0.05	0.16	0.02	0.16	0.02	5.51	2.68	0.81	1.08	24.00	1.13
XNZ5	0.28	0.44	0.07	0.34	0.07	0.07	0.11	0.02	0.14	0.80	0.03	0.10	0.02	0.13	0.02	2.64	3.82	0.72	1.02	26.67	0.54
XNZ7	0.30	0.51	0.08	0.35	0.08	0.07	0.11	0.02	0.17	0.74	0.03	0.12	0.02	0.14	0.02	2.76	3.56	0.76	1.08	24.67	0.57
XNZ8	0.18	0.35	0.05	0.26	0.06	0.06	0.08	0.02	0.11	0.58	0.03	0.09	0.02	0.11	0.02	2.02	3.52	0.85	0.94	19.33	0.55
XNZ9	0.32	1.16	0.17	1.01	0.40	0.27	0.48	0.08	0.55	2.23	0.12	0.32	0.04	0.32	0.04	7.51	3.03	1.05	0.87	18.58	1.25
XNZ12	1.43	2.74	0.44	2.24	0.58	0.45	0.97	0.17	1.07	7.53	0.25	0.71	0.10	0.66	0.10	19.44	2.92	0.79	0.99	30.12	0.88
XNZ13	N.D.	N.D.	N.D.	N.D.	N.D.	N.D.	N.D.	N.D.	N.D.	N.D.	N.D.	N.D.	N.D.	N.D.	N.D.	N.D.	N.D.	N.D.	N.D.	N.D.	N.D.
XNX2	8.09	8.62	1.43	6.61	1.36	1.11	2.09	0.31	2.04	18.34	0.51	1.54	0.21	1.41	0.23	53.90	3.47	0.58	1.07	35.96	0.96
XNX5	N.D.	N.D.	N.D.	N.D.	N.D.	N.D.	N.D.	N.D.	N.D.	N.D.	N.D.	N.D.	N.D.	N.D.	N.D.	N.D.	N.D.	N.D.	N.D.	N.D.	N.D.
XNZ14	3.11	6.14	1.02	5.14	1.32	0.56	1.61	0.30	1.89	9.31	0.42	1.24	0.18	1.25	0.19	33.68	1.81	0.78	1.01	22.17	1.06

XNZ15	N.D.	N.D.	N.D.	N.D.	N.D.	N.D.	N.D.	N.D.	N.D.	N.D.	N.D.	N.D.	N.D.	N.D.	N.D.	N.D.	N.D.	N.D.	N.D.	N.D.	N.D.

* TREY represents total concentration of rare earth elements and Y

Eu_N/Eu_N^* represents Eu anomalies normalized by PAAS

Ce_N/Ce_N^* represents Ce anomalies normalized by PAAS

Pr_N/Pr_N^* represents Pr anomalies normalized by PAAS

N. D. = Not Determined

61

62

Table S6: Hydrothermal fields and related information in the SWIR.

Name	longitude (°)	Latitude (°)	Type
SWIR, 51.7 E	51.7320	-37.4660	active, inferred
SWIR, Plume 1, Segment 17	58.5000	-31.1830	active, inferred
SWIR, Plume 5	64.4500	-27.9170	active, inferred
SWIR, 53.2 E	53.2550	-36.1010	active, inferred
SWIR, Plume 2, Segment 16	58.9670	-31.0670	active, inferred
SWIR, Plume 6	65.1330	-27.7670	active, inferred
SWIR, 63.9 E	63.9230	-27.8510	active, inferred
SWIR, Plume 3, Segment 16	59.3830	-30.8500	active, inferred
SWIR, unnamed, Segment 26	50.8527	-37.6080	active, inferred
SWIR, D9B	18.8170	-52.7070	active, inferred
SWIR, D20	22.1880	-53.0200	active, inferred
SWIR, D57	13.7380	-52.2240	active, inferred
SWIR, D36	11.7110	-52.7490	active, inferred
SWIR, D62	15.1030	-52.2530	active, inferred
SWIR, D50B	12.7480	-52.4200	active, inferred
SWIR, D82	15.5830	-52.2080	active, inferred
SWIR, D54	13.3120	-52.4370	active, inferred
Tiancheng	63.5500	-27.9670	active, confirmed
Longqi	49.6494	-37.7838	active, confirmed
Duanqiao	50.4671	-37.6579	active, inferred
Mount Jourdanne	63.9333	-27.8500	inactive
Jade Emperor Mountain	49.2600	-37.9400	inactive
Bai Causeway	48.8000	-37.9000	active, inferred

near Jade Emperor Mountain, on-axis	49.2166	-37.8666	active, inferred
Landing Stage	51.0000	-37.5000	active, inferred
Su Causeway	48.6000	-38.1000	active, inferred

These data are from Beaulieu et al. (2020).

References:

Beaulieu, S.E., Szafra, ski, K.M., 2020. InterRidge Global Database of Active Submarine Hydrothermal Vent Fields Version 3.4. PANGAEA.

Table S7: EDS data (matching with Figure 2 (E, F) and Figure S3 (B, C, E, F)).

Sample	Element	Wt %	At %
XNZ12	O	50.25	65.07
	Na	2.26	2.04
	Si	41.67	30.74
	Fe	5.81	2.16
	Matrix	Correction	ZAF
XNX1	C	65.13	-27.77
	O	10.90	20.70
	Fe	26.54	10.85
	Na	3.75	3.72
	Mg	2.43	2.28
	Si	16.73	13.60
	P	8.72	6.43
	Ag	1.41	0.30
	Matrix	Correction	ZAF
XNZ10 (Red point)	C	11.14	20.1
	O	32.14	43.54
	Fe	18.58	7.21
	Na	2.64	2.49
	Mg	2.08	1.86
	Si	22.32	17.23
	P	9.83	6.88
	K	1.27	0.7

Sample	Element	Wt %	At %
XNZ10 (Blue point)	C	16.53	28.46
	O	36.25	46.86
	Si	21.31	15.69
	Ag	2.39	0.46
	Fe	20.03	7.42
	Zn	3.49	1.1
	Matrix	Correction	ZAF
XNZ1 (Green point)	CK	14.04	23.59
	OK	42.7	53.86
	Na	4.01	3.52
	Si	7.95	5.71
	P	4.59	2.99
	S	1.08	0.68
	Cl	1.84	1.05
	Fe	23.78	8.59
	Matrix	Correction	ZAF
XNZ1 (Yellow point)	O	46.14	65.57
	Na	7.2	7.12
	Mg	2.88	2.69
	Si	12.12	9.81
	P	4.42	3.24
	Cl	2.03	1.3

	Matrix	Correction	ZAF

Fe	25.22	10.27	
Matrix	Correction	ZAF	